Cell Reports

Report

NOTCH1 Inhibits Activation of ATM by Impairing the Formation of an ATM-FOXO3a-KAT5/Tip60 Complex

Graphical Abstract

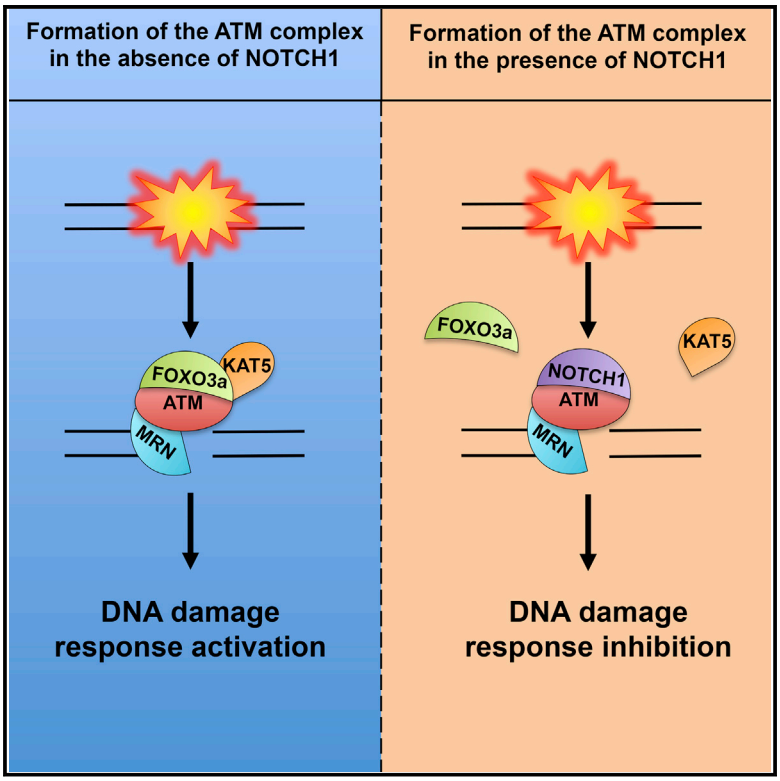

Authors

Marek Adamowicz, Jelena Vermezovic, Fabrizio d'Adda di Fagagna

Correspondence

fabrizio.dadda@ifom.eu

In Brief

Adamowicz et al. show that NOTCH1 inhibits ATM not by impairing ATM recruitment to the DSBs but by blocking formation of a three-protein complex composed of ATM, FOXO3a, and KAT5/Tip60. NOTCH1 competes with FOXO3a for binding to the FATC domain of ATM, resulting in NOTCH1-mediated ATM kinase inhibition.

Highlights

- NOTCH1 does not inhibit recruitment of ATM to DSBs
- NOTCH1 competes with FOXO3a for binding to the FATC domain of ATM
- FOXO3a is necessary for KAT5/Tip60 binding to ATM
- Induction of FOXO3a nuclear localization sensitizes TALL-1 cancer cells to DNA damage

Adamowicz et al., 2016, Cell Reports *16*, 2068–2076
August 23, 2016
http://dx.doi.org/10.1016/j.celrep.2016.07.038

CellPress

OPEN ACCESS
CellPress

Cell Reports
Report

NOTCH1 Inhibits Activation of ATM by Impairing the Formation of an ATM-FOXO3a-KAT5/Tip60 Complex

Marek Adamowicz,[1] Jelena Vermezovic,[1] and Fabrizio d'Adda di Fagagna[1,2,3,*]
[1]IFOM Foundation, FIRC Institute of Molecular Oncology Foundation, 20139 Milan, Italy
[2]Istituto di Genetica Molecolare, Consiglio Nazionale delle Ricerche, 27100 Pavia, Italy
[3]Lead Contact
*Correspondence: fabrizio.dadda@ifom.eu
http://dx.doi.org/10.1016/j.celrep.2016.07.038

SUMMARY

The DNA damage response (DDR) signal transduction pathway is responsible for sensing DNA damage and further relaying this signal into the cell. ATM is an apical DDR kinase that orchestrates the activation and the recruitment of downstream DDR factors to induce cell-cycle arrest and repair. We have previously shown that NOTCH1 inhibits ATM activation upon DNA damage, but the underlying mechanism remains unclear. Here, we show that NOTCH1 does not impair ATM recruitment to DNA double-strand breaks (DSBs). Rather, NOTCH1 prevents binding of FOXO3a and KAT5/Tip60 to ATM through a mechanism in which NOTCH1 competes with FOXO3a for ATM binding. Lack of FOXO3a binding to ATM leads to the loss of KAT5/Tip60 association with ATM. Moreover, expression of NOTCH1 or depletion of ATM impairs the formation of the FOXO3a-KAT5/Tip60 protein complex. Finally, we show that pharmacological induction of FOXO3a nuclear localization sensitizes NOTCH1-driven cancers to DNA-damage-induced cell death.

INTRODUCTION

Ataxia-telengiectasia mutated (ATM) is a phosphatidylinositol-3-like protein kinase discovered over 20 years ago (Savitsky et al., 1995). Although several reports describe the role of ATM in the DNA damage response (DDR), the underlying molecular mechanisms of ATM activation still awaits complete elucidation. It has been shown that upon DNA damage, ATM is recruited to the double-strand breaks (DSBs) (Andegeko et al., 2001) through its interaction with NBS1 (Falck et al., 2005; Nakada et al., 2003). MRE11, RAD50, and NBS1 form a protein complex known as MRN, which is one of the first to localize to DSBs (Polo and Jackson, 2011). Upon MRN-mediated ATM recruitment, a lysine acetyl-transferase 5 (also known as a Tip60, hereinafter referred to as KAT5), which binds to ATM indirectly (Sun et al., 2005, 2010), interacts with histone H3 trimethylated at lysine 9 (H3K9m3). This interaction induces acetyl-transferase activity of KAT5, which acetylates ATM (Sun et al., 2007, 2009). ATM acetylation has been proposed to be an early step in ATM activation, preceding autophosphorylation and activation (Sun et al., 2007). In addition, c-Abl-mediated phosphorylation of KAT5 was shown to be necessary for KAT5 activation in response to DNA damage (Kaidi and Jackson, 2013).

FOXO3a is a mammalian transcription factor that contains a unique DNA binding forkhead domain and belongs to the forkhead box-O family of transcription factors (Calnan and Brunet, 2008). FOXO3a is involved in many cellular processes such as cell-cycle control, apoptosis, and more recently, DDR. FOXO3a has been proposed to bind to ATM upon DNA damage and to be necessary for its activation. Lack of FOXO3a impairs both ATM autophosphorylation and phosphorylation of its substrates, although the exact mechanism of FOXO3a-mediated ATM activation remains unclear (Chung et al., 2012; Tsai et al., 2008).

NOTCH1 is a transmembrane receptor which, upon interaction with one of its ligands, is processed by gamma secretase protease (Andersen et al., 2012). The cleaved intracellular part of NOTCH1 (N1IC) released in such processes translocates to the nucleus and initiates the transcription of NOTCH1 target genes involved in cell proliferation, differentiation, and survival (Andersen et al., 2012).

We have recently discovered and reported that NOTCH1 is a direct inhibitor of ATM, independent from its transcriptional activity (Vermezovic et al., 2015). Here, we demonstrate that NOTCH1 inactivates ATM by preventing FOXO3a binding to the FRAP-ATM-TRRAP-C-terminal (FATC) domain of ATM. We show that FOXO3a is necessary for KAT5 binding to ATM and the formation of an ATM, FOXO3a, and KAT5 protein complex, hereinafter referred to as the ATM activation complex (AAC). NOTCH1-mediated FOXO3a displacement results in the impairment of KAT5-ATM interaction and ATM inactivation. Additionally, we provide evidence that the expression of NOTCH1 or lack of ATM impairs the formation of the FOXO3a-KAT5 protein complex, suggesting that the interaction between these two proteins takes place only in the context of the AAC. Finally, we show that pharmacological induction of FOXO3a nuclear localization sensitizes NOTCH1-driven cancers to DNA damage-induced cell death.

RESULTS

NOTCH1 Binding to ATM Does Not Impair Recruitment to DSBs

It has been shown that ATM interacts with NBS1 and that this allows its recruitment to DSBs (Nakada et al., 2003; Falck et al.,

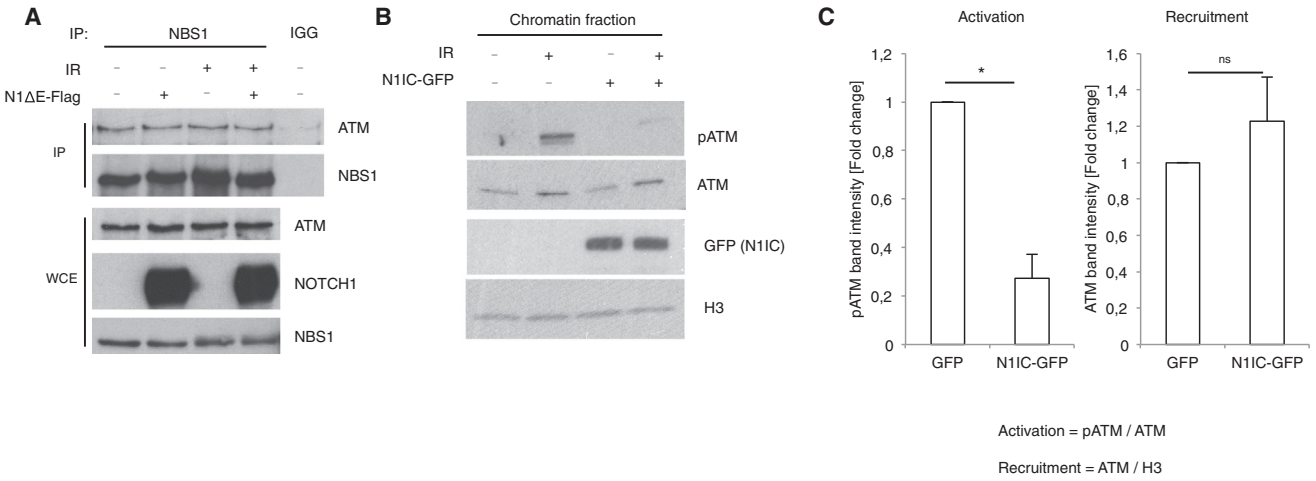

Figure 1. NOTCH1 Does Not Inhibit ATM Recruitment to DSBs

(A) CoIP of the ATM with NBS1 in cells expressing, or not expressing, NOTCH1. IGG, immunoglobulin G; WCE, whole-cell extract.

(B) Immunoblot analysis of the HEK293T cells transfected with N1IC-GFP or EGFP constructs followed by fluorescence-activated cell sorting (FACS).

(C) Quantification of the signals shown in (B). pATM signal was normalized to ATM for "ATM activation" analysis, and ATM signal was normalized to H3 signal for "ATM recruitment" analysis. In both cases, signal of NO IR samples was subtracted from IR signal (mean ± SEM; n = 3; two-tailed Student's t test; *p ≤ 0.05; ns, not significant).

2005). Therefore, we tested whether NOTCH1 expression interferes with ATM-NBS1 interaction. We immunoprecipitated NBS1 in HEK293T cell lysates expressing, or not expressing, a constitutively active form of NOTCH1 (N1ΔE-Flag) (Rustighi et al., 2009). We observed that NBS1 remains in a complex with ATM both in NOTCH1-expressing and mock-transfected cells and regardless of ionizing radiation (IR) treatment (Figure 1A). Next, we studied whether NOTCH1 expression affects ATM recruitment to chromatin. To that end, we analyzed, by immunoblotting, the chromatin fraction of lysates from cells expressing a nuclear form of NOTCH1 fused to GFP (N1IC-GFP) and treated with IR. Though ATM was inactivated, as indicated by the decreased ATM autophosphorylation on serine 1981 (pATM), we could not observe any statistical difference in ATM recruitment to chromatin upon DNA damage in N1IC-GFP-expressing cells, as compared to control cells (Figures 1B and 1C). Thus, although NOTCH1 inactivates ATM, it does not do so by inhibiting ATM recruitment to the DSBs.

FOXO3a Binds Directly to the FATC Domain of ATM

FOXO3a has been described as one of the critical protein factors necessary for ATM activation (Chung et al., 2012; Tsai et al., 2008), by virtue of its ability to directly interact with ATM (Tsai et al., 2008). To probe this interaction more in depth, we mapped the domain of ATM involved in FOXO3a binding. We performed immunoprecipitation (IP) of Myc-tagged ATM fragments, spanning the entire length of the ATM protein (Figure S1A). We observed a strong interaction between FOXO3a and a C-terminal ATM fragment (amino acids [aa] 1,965–3,056). Notably, this fragment contains the 33-aa FATC domain (aa 3,023–3,056), previously proposed as a critical domain in the regulation of ATM kinase activity (Jiang et al., 2006). To map with an increased resolution the interaction domain of ATM with FOXO3a, we incubated a lysate of cells overexpressing Myc-FOXO3a with beads bound to purified glutathione S-transferase (GST) fused to 12 individual fragments encompassing the whole ATM. We observed a specific interaction of FOXO3a with the ATM fragment spanning aa 2,842–3,056 but not with that spanning aa 2,682–3,012 (Figure 2A). The same specific interaction could also be observed when the GST-ATM fragment spanning 2,842–3,056 aa (hereinafter referred to as GST-ATM) was incubated with endogenous or recombinant purified FOXO3a, indicating that such interaction is direct (Figures S1B and S1C). To prove the essential role of the FATC domain of ATM in FOXO3a binding, we expressed a full-length ATM (wild-type [WT] ATM) or ATM lacking the FATC domain (1–2992 aa) (ATMΔFATC) in HEK293T cells. IP experiments demonstrated that the FATC domain of ATM is essential for its interaction with FOXO3a (Figure S1D).

We decided to further investigate the nature of the endogenous ATM-FOXO3a complex. We immunoprecipitated endogenous FOXO3a in lysates of cells exposed, or not exposed, to IR. We observed that FOXO3a was in a complex with ATM independently of the induction of DNA damage (Figure 2B). Next, to determine whether the entire pool of ATM protein is in a complex with FOXO3a, we performed sequential immunodepletions of either ATM or FOXO3a, followed by reciprocal immunodepletion. We observed that, despite the complete immunodepletion of ATM, the levels of FOXO3a are not dramatically affected. Differently, immunodepletion of FOXO3a led to significant ATM protein depletion (Figure S1E). This result indicates that all of ATM is in a complex with FOXO3a, while not all of FOXO3a is associated with ATM. We conclude that nuclear ATM is quantitatively bound to FOXO3a directly through its FATC domain.

NOTCH1 Competes with FOXO3a for ATM Binding

We have previously shown that NOTCH1 binds directly to the FATC domain of ATM and inactivates ATM in response to IR

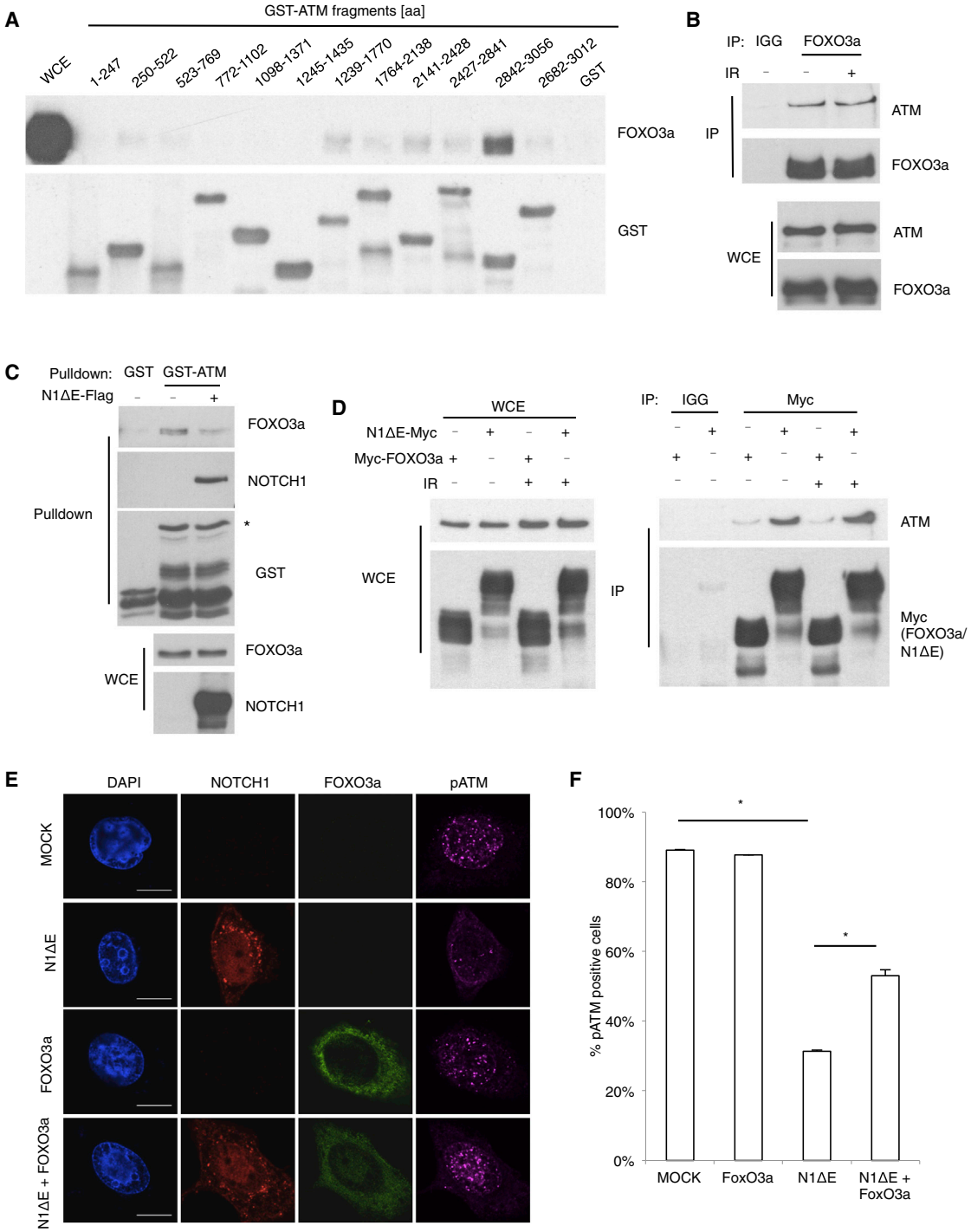

Figure 2. NOTCH1 Competes with FOXO3a for ATM Binding

(A) Immunoblot analysis of the pull-down experiments with GST or GST-ATM fragments (as indicated) incubated with lysate of HEK293T cells transfected with Myc-FOXO3a construct.

(B) Immunoblot analysis of the coIP of ATM with FOXO3a.

(C) Immunoblot analysis of the pull-down experiment with GST or GST-ATM (2,842–3,056 aa) incubated with the lysate of HEK293T (asterisk indicates correct band).

(D) Immunoblot analysis of the coIP of ATM with FOXO3a or NOTCH1 in cells overexpressing FOXO3a or expressing NOTCH1.

(E) Immunofluorescence analysis of the pATM staining in HeLa cells expressing, or not expressing, NOTCH1 or overexpressing FOXO3a (scale bars, 10 μm).

(F) Analysis of the images shown in (E). Percentage of pATM-positive cells (more than three foci) (mean ± SEM; n = 3; two-tailed Student's t test; $p \leq 0.05$).

(Vermezovic et al., 2015). Therefore, we tested whether NOTCH1 competes with FOXO3a in binding to the FATC domain of ATM. Thus, we incubated GST-ATM bound to beads with lysates from cells transfected with N1ΔE-Flag or empty vector. We observed that FOXO3a binding to FATC domain of ATM was diminished in the presence of NOTCH1 (Figure 2C). A similar conclusion was reached by studying the interaction between endogenous ATM and FOXO3a proteins by proximity ligation assay (PLA) (Figures S1F and S1G). Moreover, ATM-FOXO3a interaction was rescued in the presence of a NOTCH1 inhibitor (DAPT) (Figures S1F and S1G), which, at the same time, abolished interaction between ATM and NOTCH1 (Figures S1H and S1I). Reduced interaction between FOXO3a and ATM did not result from NOTCH1-mediated sequestration of FOXO3a, since no interaction between NOTCH1 and FOXO3a could be observed (Figure S1J). Consistently, in living cells, the overexpression of FOXO3a leads to a detectably decreased NOTCH1 and ATM interaction (Figures S1K and S1L).

Next, we compared the strength of the interactions of NOTCH1 and FOXO3a to ATM. To do that, we transfected either Myc-FOXO3a or N1ΔE-Myc and performed an IP of the Myc-tagged proteins. We observed that NOTCH1 was binding more efficiently to ATM than FOXO3a (Figure 2D). This was not due to the differential distribution of expressed tagged proteins in distinct cellular compartments (Figure S1M). Moreover, IP of NOTCH1 or FOXO3a from the nuclear fraction confirmed the results obtained in whole-cell extracts (Figures S1N and S1O).

Next, we asked whether overexpression of FOXO3a could rescue NOTCH1-driven inhibition of ATM activation upon IR. We observed an inhibition of ATM activation, as judged by the inhibition of pATM foci formation, in cells expressing NOTCH1 but not FOXO3a. Furthermore the overexpression of FOXO3 together with NOTCH1 rescues NOTCH1-mediated ATM inactivation (Figures 2E and 2F).

We concluded that NOTCH1 competes with FOXO3a for the FATC domain of ATM and binds to it with higher strength.

KAT5 Binds to ATM through FOXO3a

The role of FOXO3a in the activation of ATM remains unclear. Our results indicate that FOXO3a binds directly to the FATC domain of ATM and that all of ATM is in a complex with it (Figures 2 and S1). Next, we asked whether FOXO3a can form a protein complex with KAT5, which has been reported to bind to the FATC domain of ATM, although indirectly and independently of DNA damage (Sun et al., 2010) (Figure S2A). We immunoprecipitated FOXO3a from cell lysates, and we detected KAT5 in a complex with FOXO3a in cells exposed, or not exposed, to IR (Figure 3A). In order to exclude the possibility of DNA potentially bridging the two proteins, we performed the same IP in the presence or absence of benzonase nuclease, and this did not affect the interaction between KAT5 and FOXO3a (Figure S2B). To test whether such interaction was direct, we performed a pull-down experiment with recombinant purified proteins GST-KAT5 and FOXO3a: we observed that KAT5 and FOXO3a can, indeed, bind directly to each other (Figure S2C).

Next, we aimed at mapping the protein domains of KAT5 and FOXO3a involved in such interaction. We expressed three sequential Myc-tagged fragments of FOXO3a spanning its whole length (Figure S2D; fragments 1–3) in HEK293T cells, followed by IP with anti-Myc antibodies. We observed a specific binding of KAT5 to the C-terminal part of FOXO3a (500–673 aa) (Figure S2E). To define more precisely the domain in the C-terminal region of FOXO3a involved in KAT5 binding, we generated two different C-terminal fragments of FOXO3a (Figure S2D; fragments 4–5). IP of FOXO3a (fragments 3–5) showed that KAT5 binds to FOXO3a in the C-terminal region, between 620 and 650 aa (Figure S2F).

Next, by using four different constructs spanning the entire length of KAT5 (Figure S2G; fragments 1–4), we aimed at mapping the interaction domains between KAT5 and FOXO3a and between KAT5 and ATM. We performed IPs in cells expressing Flag-tagged fragments of KAT5 (1–4). We observed that both FOXO3a and ATM were binding specifically to the C-terminal part of KAT5 (285–513 aa) (Figures S2H and S2I). In addition, we expressed in cells the very C-terminal part of KAT5 (450–513 aa), and we were able to observe both ATM as well as FOXO3a binding to it (Figure S2J).

Given that KAT5 was reported to bind to ATM indirectly, we tested whether FOXO3a was necessary for the binding of KAT5 to ATM. We transfected cells with small interfering RNA (siRNA) against *FOXO3a* (siFOXO3a) or siRNA targeting *LUCIFERASE* (control). We observed that, as previously reported (Tsai et al., 2008), cells knocked down for FOXO3a displayed an impaired activation of ATM, as shown by reduced pATM signal (Figure S2K). Next, to assess the interaction between ATM and KAT5, we immunoprecipitated KAT5. Surprisingly, in the absence of FOXO3a also, the interaction between KAT5 and ATM was impaired as compared to mock-transfected cells (Figures 3B and S2L).

Unexpectedly, we observed that reduction of ATM-KAT5 interaction in the cells treated with siRNA against *FOXO3a* was partial. Therefore, we asked whether other FOXO family members, such as FOXO1 and FOXO4, could contribute to the binding of ATM and KAT5 in the absence of FOXO3a considering high conservation of C-terminal region (Figure S2M). Therefore, we immunoprecipitated FOXO1 and FOXO4, and we observed that ATM was able to form a protein complex with both of them (Figures S2N and S2O). Moreover, the IP of KAT5 showed that FOXO1 and FOXO4 can bind to KAT5 (Figure S2P). Finally, we also observed that knockdown of *FOXO3a* results in increased levels of endogenous FOXO4 (Figure S2Q). To overcome a problem of potential redundancy between FOXO3a, FOXO1, and FOXO4, we performed an in vitro binding assay. We incubated GST-ATM with recombinant KAT5 and recombinant FOXO3a. As previously shown (Sun et al., 2010), we could not detect any direct interaction between GST-ATM and recombinant KAT5, but in the presence of recombinant FOXO3a, the binding between ATM and KAT5 became evident, demonstrating that FOXO3a can mediate the interaction between ATM and KAT5 (Figure 3C).

Next, we checked whether the formation of the AAC is affected by the presence of DNA damage and whether its formation changes with the cell-cycle progression. Therefore, we performed PLA between the three components of the AAC in cells exposed, or not exposed, to IR. We could not observe any

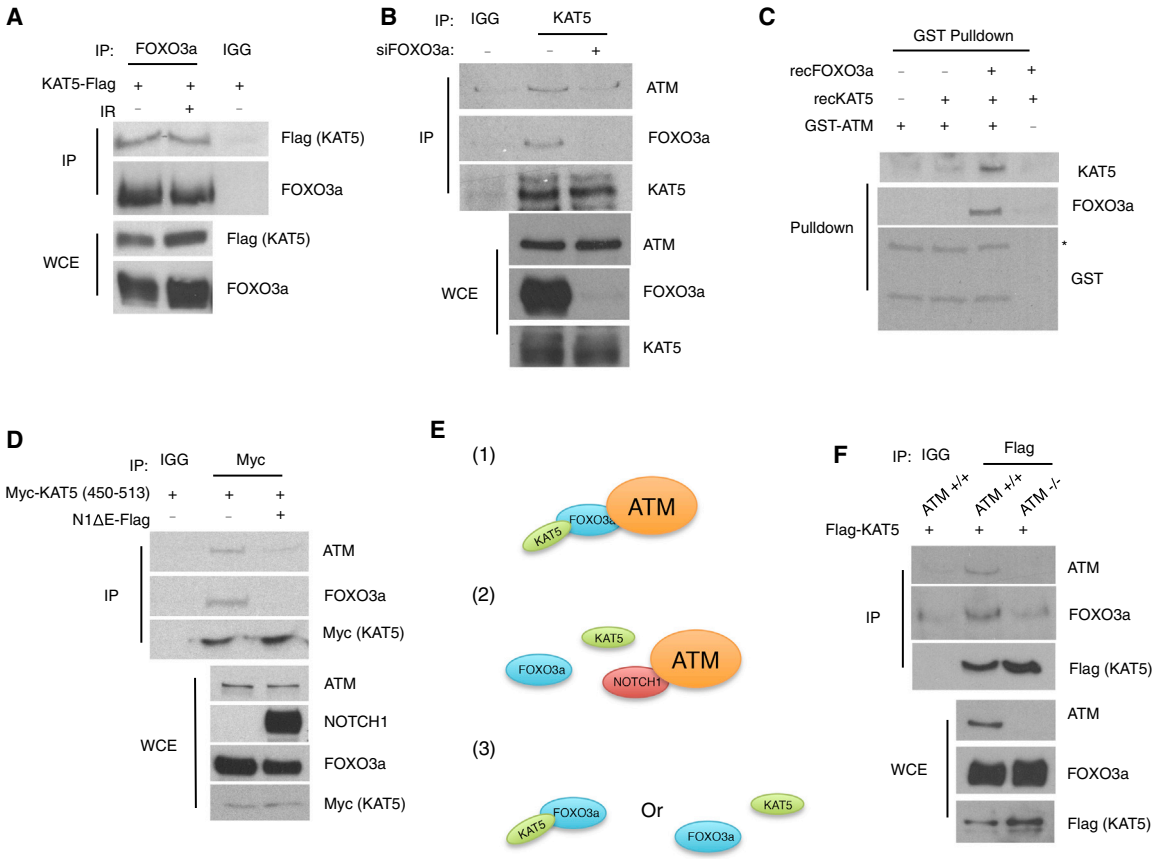

Figure 3. FOXO3a Bridges KAT5 Binding to ATM

(A) Immunoblot analysis of the coIP of KAT5 with FOXO3a.

(B) Immunoblot analysis of the coIP of ATM and FOXO3a with KAT5 in cells treated, or not treated, with siRNA against *FOXO3a*.

(C) Immunoblot analysis of the pull-down experiment with GST-ATM (2,842–3,056 aa) incubated as indicated with the recombinant human KAT5 and recombinant human FOXO3a proteins (asterisk indicates correct band).

(D) Immunoblot analysis of the coIP of ATM and FOXO3a with Myc-KAT5 fragment (450–513 aa) in the presence or absence of NOTCH1.

(E) Three schemes showing the potential interactions among AAC components: (1) AAC complex; (2) AAC complex in the presence of NOTCH1; (3) two possibilities of FOXO3a-KAT5 interaction in the absence of ATM.

(F) Immunoblot analysis of the coIP of FOXO3a and ATM with KAT5.

changes in the interaction between AAC components in the presence or absence of DNA damage (Figures S2R–S2W). Next, to check whether the formation of the AAC is differentially modulated during the cell cycle, we performed PLA in HeLa Fucci cells (Sakaue-Sawano et al., 2008). We observed a modest but reproducible increase in the interactions of all AAC components in the S/G2 phase compared to the G1 phase of the cell cycle (Figures S2X–S2AC). Similar to the observed changes in the interactions between AAC components, we observed an increase of ATM autophosphorylation in cells in the S/G2 phase of the cell cycle (Figures S2AD and S2AE). Results consistent with ours were reported by Pandita et al. (2000), who observed increased ATM activation upon IR in S-phase cells as compared to G1 and G2.

Our results demonstrate that NOTCH1 perturbs the binding of FOXO3a to ATM. Since KAT5 binds to FOXO3a, we asked whether NOTCH1 has an impact on KAT5 association with ATM. We immunoprecipitated Myc-tagged KAT5 in cells expressing NOTCH1 or mock-transfected cells. We observed that NOTCH1 expression perturbed binding of KAT5 to ATM, as compared to the control (Figure 3D). Surprisingly, we observed that expression of NOTCH1 impaired the binding of KAT5 not only to ATM but also to FOXO3a (Figure 3D). As we have already excluded the possibility that NOTCH1 could sequester FOXO3a (Figure S1J), we hypothesized that the interaction between FOXO3a and KAT5 may take place only in the context of the formation of the AAC (Figure 3E). To test this hypothesis, we performed an IP of Flag-tagged KAT5 in either WT or *Atm* knockout mouse embryonic stem cells (mESCs). Indeed, in the absence of ATM, we could not detect any interaction between KAT5 and FOXO3a (Figure 3F).

We propose that KAT5, FOXO3a, and ATM form the AAC, which is perturbed by NOTCH1 binding to ATM and that this interaction between FOXO3a and KAT5 is restricted to the formation of the AAC.

Induction of FOXO3a Nuclear Localization Sensitizes TALL Cells to DNA-Damage-Mediated Apoptosis

T cell acute lymphoblasic leukemia (TALL) cancer cells carry mutations in the *NOTCH1* gene that result in increased expression and activity of NOTCH1 (Ferrando, 2009). We have previously shown that treatment of TALL-1 cells with gamma-secretase inhibitor (GSI; a widely used NOTCH1 inhibitor that prevents its nuclear translocation) leads to increased activation of DDR signaling and ensuing DDR-induced cell death (Vermezovic et al., 2015). Consequently, we decided to test whether GSI treatment of TALL cells has an impact on the formation of the AAC. To that end, we used CUTLL1 cells that express high levels of NOTCH1. GSI treatment of CUTLL1 cells caused a decrease of the nuclear form of NOTCH1 as well as of the interaction between ATM and NOTCH1 (Figures S3A–S3C). Next, we performed PLA between ATM and FOXO3a as well as FOXO3a and KAT5 in GSI-treated cells. We observed that inhibition of NOTCH1 resulted in the increase of the interaction between ATM and FOXO3a as well as that between FOXO3a and KAT5 (Figures S3D–S3G).

On the basis of the results showing that NOTCH1 expression in TALL cells leads to the impairment of the AAC formation, we asked whether we can rescue NOTCH1-mediated ATM inactivation in the TALL cells by increasing levels of FOXO3a in the nucleus. Therefore, we tested whether the induced translocation of FOXO3a into the nuclei of TALL-1 cells would have an impact on ATM activation as well as their survival after exposure to IR. We pretreated TALL-1 cells with metformin (MET), which, by acting through AMPK, induces FOXO3a nuclear import (Hu et al., 2014). To confirm the effect of MET, we analyzed the expression levels of FOXO3a target gene (*GADD45α*). We observed that MET treatment resulted in FOXO3a nuclear accumulation in TALL-1 cells (Figures S3H and S3I). Next, we analyzed the effect of MET on TALL-1 cells subjected to IR. Pretreatment with MET resulted in an increase of ATM activation (pATM) upon IR as compared to mock-treated cells (Figure 4A; Figure S3J). Moreover, we observed an increase of DDR-induced cell death in MET-treated cells (Figure 4B). As FOXO3a is not a direct target of MET, we sought to modulate an independent pathway that has an impact on FOXO3a nuclear localization. For this purpose, we tested the impact of pharmacological inhibition of p38 on TALL-1 cells by the use of a p38 kinase inhibitor (SB203580; hereinafter referred to as SB) previously shown to induce FOXO3a nuclear localization in treated cells (Clavel et al., 2010). We pretreated TALL-1 cells with SB and exposed them to IR. We observed an increase of FOXO3a nuclear import as judged by augmented transcription of a FOXO3a target gene (Figure S3K) and FOXO3a nuclear localization (Figure S3L). Furthermore, we observed that SB pretreatment increased ATM activation (pATM), as well as IR-induced cell death, when compared to mock-treated cells (Figures 4C, S3M, and S3N) and that cell death was dependent on ATM activation (Figure S3O).

We conclude that induction of FOXO3a nuclear localization sensitizes TALL-1 cells to DNA damage-induced cell death.

DISCUSSION

DDR is one of the most important signaling pathways in the cell, and it is responsible for the maintenance of genome integrity. Here we show that NOTCH1 inhibits DDR by impairing the formation of the AAC composed from ATM, FOXO3a, and KAT5. Our results reveal a hitherto-unknown complex modulation of ATM kinase activity between two factors interacting with ATM.

It has been shown that NBS1-ATM interaction is crucial for the MRN-mediated ATM recruitment to DSBs (Falck et al., 2005; Nakada et al., 2003). Although NBS1 interacts with N-terminal part of ATM, it has been reported that point mutations in the FATC domain of ATM can affect NBS1 binding to ATM and, subsequently, ATM localization at DSBs (You et al., 2005; Ogi et al., 2015). We found that NOTCH1 interacts with ATM through the FATC domain (Vermezovic et al., 2015), but we did not observe any impairment in NBS1 binding to ATM or in its recruitment to DSBs. We show that ATM in the presence of NOTCH1 can localize at the DSB site but that it does not undergo autophosporylation; this is consistent with some recent published data (Hartlerode et al., 2015; Yamamoto et al., 2012). Differently, others reported that autophosphorylation is necessary for ATM retention at DSBs (So et al., 2009), which underlies our still-incomplete understanding of the full impact of ATM autophosphorylation on its activation and recruitment to DSBs.

FOXO3a has been shown to interact with ATM upon DNA damage (Tsai et al., 2008). We demonstrate that FOXO3a interacts with ATM independently of the presence of DNA damage. It has been shown that FOXO3a binds to ATM in a domain spanning 1,764–2,841 aa. Although we did observe FOXO3a binding to this domain, we detected a binding of higher affinity with the 2,842–3,056 aa GST-ATM fragment, which has not been tested in the previously published study (Tsai et al., 2008).

The exact function of FOXO3a in ATM activation was unclear thus far. Here, we propose that FOXO3a participates in the process of ATM activation by bridging KAT5 to ATM. Previous studies have shown that KAT5-ATM interaction is mediated by the FATC domain of ATM and that such binding is indirect, suggesting the existence of one or more bridging proteins (Sun et al., 2005, 2010). Consistent with this observation, we show that FOXO3a, like KAT5, binds specifically to the FATC domain of ATM, but unlike with KAT5, the observed binding is direct. Unexpectedly, we discovered that FOXO3a interacts directly with KAT5, and, in the absence of FOXO3a, KAT5 loses its ability to bind to ATM. It is noteworthy that we observed that the FOXO3a paralogues FOXO1 and FOXO4 could play a similar role in the absence of FOXO3a. Consistent with this, it has been shown before that another FOX family member, FOXP3, can interact with KAT5 (Li et al., 2007).

The interaction between FOXO3a and KAT5 seems to be restricted to the formation of the AAC, since, both in the absence of ATM and upon expression of NOTCH1, an interaction between FOXO3a and KAT5 cannot be detected. Based on that, we would like to propose a model in which ATM activation is dependent on the formation of the AAC, which consists of KAT5, FOXO3a, and ATM proteins. Formation of this three-protein complex allows proper ATM activation upon DNA damage (Figure 4E).

We have already shown that IR can be combined with GSI to sensitize TALL cells to IR-mediated cell death (Vermezovic

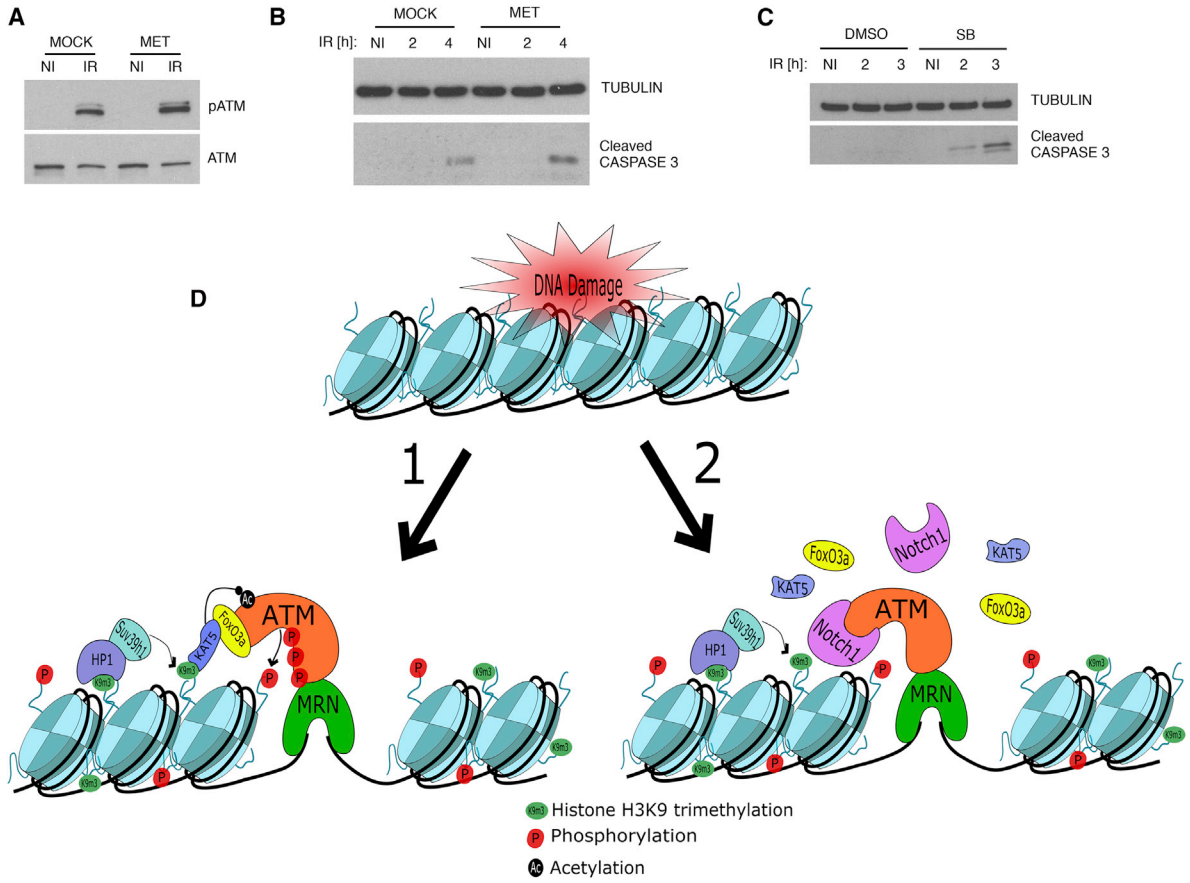

Figure 4. Induction of FOXO3a Nuclear Localization Sensitizes TALL Cells to DNA-Damage-Induced Cell Death

(A) Immunoblot analysis of the ATM activation (pATM) in TALL-1 cells pretreated with MET followed by IR.

(B) Immunoblot analysis of the DNA-damage-induced cell death (cleaved caspase-3) in TALL-1 cells pretreated with MET, followed by IR.

(C) Immunoblot analysis of the DNA-damage-induced cell death (cleaved caspase-3) in TALL-1 cells pretreated with SB, followed by IR.

(D) Model of the NOTCH1-mediated inactivation of ATM upon DNA damage. (1) ATM is recruited to DSB by its interaction with the MRN complex. Upon recruitment of ATM to DSB, KAT5, by interacting with ATM through FOXO3a, binds to H3K9m3 generated by SUV39h1 methyl-transferase, becomes activated, and acetylates ATM. This leads to ATM activation by autophosphorylation. (2) In the presence of NOTCH1, although ATM is still recruited to DSBs, NOTCH1-mediated disruption of the KAT5-FOXO3a-ATM complex results in the lack of KAT5-mediated acetylation of ATM and consequent activation.

NI, not irradiated.

et al., 2015). Here, we demonstrate the opportunity to use MET and SB to induce FOXO3a nuclear localization and sensitize TALL cells to genotoxic treatments. Our results are consistent with the previous observation that MET stimulates ATM activation in a FOXO3a-dependent manner (Vazquez-Martin et al., 2011; Hu et al., 2014).

EXPERIMENTAL PROCEDURES

Cell Culture and Treatments

HEK293T cells (Interlab Cell Line Collection) were grown in DMEM supplemented with 10% fetal bovine serum (FBS), penicillin/streptomycin, and L-glutamine. HeLa Fucci cells (RIKEN BioResource Center cell bank) (Sakaue-Sawano et al., 2008) were grown in DMEM supplemented with 10% FBS, penicillin/streptomycin, and L-glutamine. HeLa cells (ATCC) were grown in DMEM with GlutaMAX supplemented with 10% FBS, penicillin/streptomycin, and nonessential aa. TALL-1 cells (DSMZ) were grown in RPMI 1640 supplemented with 15% FBS, penicillin/streptomycin, and L-glutamine. CUTLL1 cells (a kind gift from A. Ferrando) (Palomero et al., 2006) were grown in RPMI 1640 and supplemented with 10% FBS, penicillin/streptomycin, and L-glutamine. WT mESCs and ATM KO cells (Xu and Baltimore, 1996) were grown in DMEM with Glutamax (supplemented with 15% FBS, penicillin/streptomycin, nonessential aa, sodium pyruvate, leukemia inhibitory factor, and β-mercaptoethanol). HeLa cells were transfected with the use of lipofectamine (Invitrogen), according to the manufacturer's protocol. HEK293T cells were transfected with the use of calcium phosphate. The GSI DAPT (N-[N-(3,5-difluorophenacetyl)-L-alanyl]-S-phenylglycine t-butyl ester) (Sigma) was used at a 10-μM concentration for 16 hr. CUTLL1 cells were treated with 1 μM Compound E (Calbiochem) for 24 hr before fixation. KU60019 (SelleckChem) was used at the concentration of 10 μM for 16 hr before IR. SB203580 (Jena Bioscience) was used at the concentration of 10 μM for 24 hr before the IR. MET (Tocris) was used at the concentration of 500 μM 24 hr before IR. Cells were irradiated with an X-ray machine (Faxitron): 2 Gy, 1 hr, for immunofluorescence experiments; 5 Gy, 1 hr, for immunoblot analysis of DDR activation; and 10 Gy for DDR-induced cell-death analysis. For the knockdown experiments, 20 nM siRNA (GE Dharmacon) against human *FOXO3a* was transfected with the use of RNAiMAX lipofectamine (Invitrogen) 48 hr before the experiment.

For the purpose of cell sorting, HEK293T cells were transfected with N1IC-GFP or EGFP construct and FACS sorted 1 day after for GFP. Next, cells were plated and, 8 hr later, subjected to IR (10G for recruitment experiments).

Statistical Analysis

All data are represented as means ± SEM. Statistical analysis was performed with the use of a two-tailed Student's t test. An asterisk indicates $p < 0.05$.

For more details, please see the Supplemental Experimental Procedures.

SUPPLEMENTAL INFORMATION

Supplemental Information includes Supplemental Experimental Procedures, three figures, and two tables and can be found with this article online at http://dx.doi.org/10.1016/j.celrep.2016.07.038.

AUTHOR CONTRIBUTIONS

M.A., J.V., and F.d'A.d.F. designed the study. M.A. performed all experiments. M.A., J.V., and F.d'A.d.F. analyzed the data and wrote the manuscript.

ACKNOWLEDGMENTS

We would like to thank: A. Sarin (National Centre for Biological Sciences), P.P. Di Fiore (IFOM), G. Del Sal (University of Trieste), S.P. Jackson (Gurdon Institute), K. Yamamoto (Nagasaki University), H.S. Park (Chonnam National University), M. Kastan (Duke Cancer Institute), S.J. Kim (CHA University), B. Amati (Italian Institute of Technology), Yang Xu (University of California, San Diego), Mario Cinquanta (Cogentech), and A. Behrens (Francis Crick Institute) for reagents; F. Kobia (IFOM) and V. Costanzo (IFOM) for advice; and M. Mapelli and S. Pasqualato (Istituto Europeo di Oncologia) for their help and advice regarding protein purification. F.d'A.d.F. is supported by the Fondazione Italiana per la Ricerca sul Cancro, AIRC (application 12971), Human Frontier Science Program (contract RGP 0014/2012), Cariplo Foundation (grant 2010.0818), Association for International Cancer Research (14-1331), Progetti di Ricerca di Interesse Nazionale (PRIN) 2010–2011, the Italian Ministry of Education Universities and Research EPIGEN Project, and a European Research Council advanced grant (322726).

Received: February 28, 2016
Revised: May 24, 2016
Accepted: July 14, 2016
Published: August 11, 2016

REFERENCES

Andegeko, Y., Moyal, L., Mittelman, L., Tsarfaty, I., Shiloh, Y., and Rotman, G. (2001). Nuclear retention of ATM at sites of DNA double strand breaks. J. Biol. Chem. *276*, 38224–38230.

Andersen, P., Uosaki, H., Shenje, L.T., and Kwon, C. (2012). Non-canonical Notch signaling: emerging role and mechanism. Trends Cell Biol. *22*, 257–265.

Calnan, D.R., and Brunet, A. (2008). The FoxO code. Oncogene *27*, 2276–2288.

Chung, Y.M., Park, S.H., Tsai, W.B., Wang, S.Y., Ikeda, M.A., Berek, J.S., Chen, D.J., and Hu, M.C. (2012). FOXO3 signalling links ATM to the p53 apoptotic pathway following DNA damage. Nat. Commun. *3*, 1000.

Clavel, S., Siffroi-Fernandez, S., Coldefy, A.S., Boulukos, K., Pisani, D.F., and Dérijard, B. (2010). Regulation of the intracellular localization of Foxo3a by stress-activated protein kinase signaling pathways in skeletal muscle cells. Mol. Cell. Biol. *30*, 470–480.

Falck, J., Coates, J., and Jackson, S.P. (2005). Conserved modes of recruitment of ATM, ATR and DNA-PKcs to sites of DNA damage. Nature *434*, 605–611.

Ferrando, A.A. (2009). The role of NOTCH1 signaling in T-ALL. Hematology Am. Soc. Hematol. Educ. Program *2009*, 353–361.

Hartlerode, A.J., Morgan, M.J., Wu, Y., Buis, J., and Ferguson, D.O. (2015). Recruitment and activation of the ATM kinase in the absence of DNA-damage sensors. Nat. Struct. Mol. Biol. *22*, 736–743.

Hu, T., Chung, Y.M., Guan, M., Ma, M., Ma, J., Berek, J.S., and Hu, M.C. (2014). Reprogramming ovarian and breast cancer cells into non-cancerous cells by low-dose metformin or SN-38 through FOXO3 activation. Sci. Rep. *4*, 5810.

Jiang, X., Sun, Y., Chen, S., Roy, K., and Price, B.D. (2006). The FATC domains of PIKK proteins are functionally equivalent and participate in the Tip60-dependent activation of DNA-PKcs and ATM. J. Biol. Chem. *281*, 15741–15746.

Kaidi, A., and Jackson, S.P. (2013). KAT5 tyrosine phosphorylation couples chromatin sensing to ATM signalling. Nature *498*, 70–74.

Li, B., Samanta, A., Song, X., Iacono, K.T., Bembas, K., Tao, R., Basu, S., Riley, J.L., Hancock, W.W., Shen, Y., et al. (2007). FOXP3 interactions with histone acetyltransferase and class II histone deacetylases are required for repression. Proc. Natl. Acad. Sci. USA *104*, 4571–4576.

Nakada, D., Matsumoto, K., and Sugimoto, K. (2003). ATM-related Tel1 associates with double-strand breaks through an Xrs2-dependent mechanism. Genes Dev. *17*, 1957–1962.

Ogi, H., Goto, G.H., Ghosh, A., Zencir, S., Henry, E., and Sugimoto, K. (2015). Requirement of the FATC domain of protein kinase Tel1 for localization to DNA ends and target protein recognition. Mol. Biol. Cell *26*, 3480–3488.

Palomero, T., Barnes, K.C., Real, P.J., Glade Bender, J.L., Sulis, M.L., Murty, V.V., Colovai, A.I., Balbin, M., and Ferrando, A.A. (2006). CUTLL1, a novel human T-cell lymphoma cell line with t(7;9) rearrangement, aberrant NOTCH1 activation and high sensitivity to gamma-secretase inhibitors. Leukemia *20*, 1279–1287.

Pandita, T.K., Lieberman, H.B., Lim, D.S., Dhar, S., Zheng, W., Taya, Y., and Kastan, M.B. (2000). Ionizing radiation activates the ATM kinase throughout the cell cycle. Oncogene *19*, 1386–1391.

Polo, S.E., and Jackson, S.P. (2011). Dynamics of DNA damage response proteins at DNA breaks: a focus on protein modifications. Genes Dev. *25*, 409–433.

Rustighi, A., Tiberi, L., Soldano, A., Napoli, M., Nuciforo, P., Rosato, A., Kaplan, F., Capobianco, A., Pece, S., Di Fiore, P.P., and Del Sal, G. (2009). The prolyl-isomerase Pin1 is a Notch1 target that enhances Notch1 activation in cancer. Nat. Cell Biol. *11*, 133–142.

Sakaue-Sawano, A., Kurokawa, H., Morimura, T., Hanyu, A., Hama, H., Osawa, H., Kashiwagi, S., Fukami, K., Miyata, T., Miyoshi, H., et al. (2008). Visualizing spatiotemporal dynamics of multicellular cell-cycle progression. Cell *132*, 487–498.

Savitsky, K., Bar-Shira, A., Gilad, S., Rotman, G., Ziv, Y., Vanagaite, L., Tagle, D.A., Smith, S., Uziel, T., Sfez, S., et al. (1995). A single ataxia telangiectasia gene with a product similar to PI-3 kinase. Science *268*, 1749–1753.

So, S., Davis, A.J., and Chen, D.J. (2009). Autophosphorylation at serine 1981 stabilizes ATM at DNA damage sites. J. Cell Biol. *187*, 977–990.

Sun, Y., Jiang, X., Chen, S., Fernandes, N., and Price, B.D. (2005). A role for the Tip60 histone acetyltransferase in the acetylation and activation of ATM. Proc. Natl. Acad. Sci. USA *102*, 13182–13187.

Sun, Y., Xu, Y., Roy, K., and Price, B.D. (2007). DNA damage-induced acetylation of lysine 3016 of ATM activates ATM kinase activity. Mol. Cell. Biol. *27*, 8502–8509.

Sun, Y., Jiang, X., Xu, Y., Ayrapetov, M.K., Moreau, L.A., Whetstine, J.R., and Price, B.D. (2009). Histone H3 methylation links DNA damage detection to activation of the tumour suppressor Tip60. Nat. Cell Biol. *11*, 1376–1382.

Sun, Y., Jiang, X., and Price, B.D. (2010). Tip60: connecting chromatin to DNA damage signaling. Cell Cycle *9*, 930–936.

Tsai, W.B., Chung, Y.M., Takahashi, Y., Xu, Z., and Hu, M.C. (2008). Functional interaction between FOXO3a and ATM regulates DNA damage response. Nat. Cell Biol. *10*, 460–467.

Vazquez-Martin, A., Oliveras-Ferraros, C., Cufí, S., Martin-Castillo, B., and Menendez, J.A. (2011). Metformin activates an ataxia telangiectasia mutated (ATM)/Chk2-regulated DNA damage-like response. Cell Cycle *10*, 1499–1501.

Vermezovic, J., Adamowicz, M., Santarpia, L., Rustighi, A., Forcato, M., Lucano, C., Massimiliano, L., Costanzo, V., Bicciato, S., Del Sal, G., and d'Adda di Fagagna, F. (2015). Notch is a direct negative regulator of the DNA-damage response. Nat. Struct. Mol. Biol. *22*, 417–424.

Xu, Y., and Baltimore, D. (1996). Dual roles of ATM in the cellular response to radiation and in cell growth control. Genes Dev. *10*, 2401–2410.

Yamamoto, K., Wang, Y., Jiang, W., Liu, X., Dubois, R.L., Lin, C.S., Ludwig, T., Bakkenist, C.J., and Zha, S. (2012). Kinase-dead ATM protein causes genomic instability and early embryonic lethality in mice. J. Cell Biol. *198*, 305–313.

You, Z., Chahwan, C., Bailis, J., Hunter, T., and Russell, P. (2005). ATM activation and its recruitment to damaged DNA require binding to the C terminus of Nbs1. Mol. Cell. Biol. *25*, 5363–5379.

Cell Reports, Volume *16*

Supplemental Information

NOTCH1 Inhibits Activation of ATM by Impairing the Formation of an ATM-FOXO3a-KAT5/Tip60 Complex

Marek Adamowicz, Jelena Vermezovic, and Fabrizio d'Adda di Fagagna

Supplementary inventory:

1)Supplementary experimental procedures

2)Supplementary Figures legends

3)Supplementary Figure 1A-O - related to Figure2

4)Supplementary Figure 2A-AE - related to Figure3

5)Supplementary Figure 3A-O - related to Figure4

6)Supplementary Table 1

7)Supplementary Table 2

Supplementary experimental procedures

Immunoblots and immunoprecipitations

Cells were harvested and lysed in the TEB150 lysis buffer (50 mM HEPES pH 7.4, 150 mM NaCl, 2 mM $MgCl_2$, 5 mM EGTA pH 8, 1 mM dithiothreitol (DTT), 0.5% Triton X-100, 10% glycerol, protease inhibitor cocktail set III (Calbiochem)) followed by centrifugation. For immunoprecipitation 1mg or more of protein lysate was incubated with appropriated antibody or IGGs over night (Supplementary Table 1) followed by crosslinking with Protein G (Zymed Laboratories) and subsequently washed 3 times with the lysis buffer.

For pull down experiments 1mg of lysed cells or 1ug of recombinant proteins were incubated with the GST tagged proteins bound to glutathione sepharose beads (GE Healthcare) for 2h followed by 3 washes with the lysis buffer.

Obtained samples were subjected to SDS-PAGE followed by protein transfer. Nitrocelluose membranes were next blocked in 5% milk TBS-Tween (0.1%) solution and incubated with appropriated antibodies (Supplementary Table 1).

For the purpose of cell lysate fractionation cells were incubated with Nuclear isolation buffer (0.25M Sucrose, 10mM Tris HCl pH 7.4, 5mM $MgCl_2$ supplemented with protease inhibitor cocktail set III (Calbiochem)) washed and lysed in Nuclear lysis buffer (NLB) (150mM KCl, 25mM Tris HCl pH 7.4, 5mM $MgCl_2$ and 0.5% NP40, protease inhibitor cocktail set III (Calbiochem)). Next not soluble fraction (chromatin) was spun and lysed with NLB with Benzonase nuclease (Sigma) (1:300).

Immunofluorescence and PLA

Cells were fixed with Methanol-Acetone solution (1:1) for 2min at room temperature (RT). Next cells were blocked with PBG (0.2% cold-water-fish gelatin and 0.5% BSA in PBS) followed by incubation with primary antibody for 1h at RT. Samples were subsequently washed 3 times with PBS and incubated with secondary antibody, followed by DAPI counterstaining and washing (3 times). Images were acquired with the use of wide-filed microscope (Olympus).

PLA was done accordingly to the manufactures protocol. For this purpose cells were fix in 4% PFA solution in PBS for 10min. Cytospin of CUTLL1 cells, followed by the PLA was performed as described previously (Vermezovic et al., 2015). For the PLA between ATM and NOTCH1 anti-ATM and anti-N1IC antibody were used; anti-NOTCH1 antibody was used in parallel to detect NOTCH1 positive cells. The anti-KAT5 antibody used for all of the PLA assays was kindly provided by B. Amati (Italian Institute of Technology)(Frank et al., 2003).

Constructs and protein purification

Human N1IC-GFP and EGFP constructs were a kind gift of A. Sarin (National Centre for Biological Sciences). Human N1ΔE-Flag construct were a kind gift of P.P. Di Fiore (Istituto Europeo di Oncologia). Human N1ΔE-Myc construct was a kind gift of G. Del Sal (University of Trieste). Human Flag-KAT5 construct was a kind gift of S.P. Jackson (Gurdon Institute)(Kaidi and Jackson, 2013). Human Myc-FOXO3a construct was a kind gift of K. Yamamoto (Nagasaki University) (Wang et al., 2008). Mouse 3xFlag-KAT5 fragments were a kind gift of H. S. Park (Chonnam National University)(Kim et al., 2007). Human Flag-ATM construct was a kind gift of M. Kastan (Duke cancer institute). Human Flag-ATMΔFATC (1-2992aa) was cloned by IFOM Biochemistry unit. Human Myc-ATM fragments were a kind gift of S. J. Kim (CHA University)(Park et al., 2015). GST-ATM fragments were kind gift of A. Behrens (Francis Crick Institute)(Khanna et al., 1998). Myc-KAT5 450-513aa and Myc-FOXO3a fragments (1-300aa; 1-500aa; 500-673aa; 500-650aa and 500-620aa) were amplified with the use of indicated primers (Supplementary Table 2) and cloned into BamHI and XhoI sites of pcDNA-Myc (Wang et al., 2008). GST-KAT5 and GST-FOXO3a were amplified with the use of indicated primers (Supplementary Table 2) and cloned into pGex 2rbs.

Recombinant proteins: GST-ATM fragments, GST-KAT5 and GST-FOXO3a were expressed and purified from *Esherichia Coli* BL21 bacteria with the use of Gluthatione sepharose beads (GE Healthcare). For the purpose of some experiments GST tag was cleaved with the use of Precission protease.

qRT-PCR

Total RNA was extracted from cells with the use of QIAGEN RNA extraction kit, according to manufacture procedures. RNA was subsequently retrotranscribed with the use of SuperScript Vilo kit (Invitrogen). Next cDNA was used in the RT-qPCR reaction with the use of indicated primers (Supplementary Table 2) and GoTaq q-PCR Master Mix (Promega).

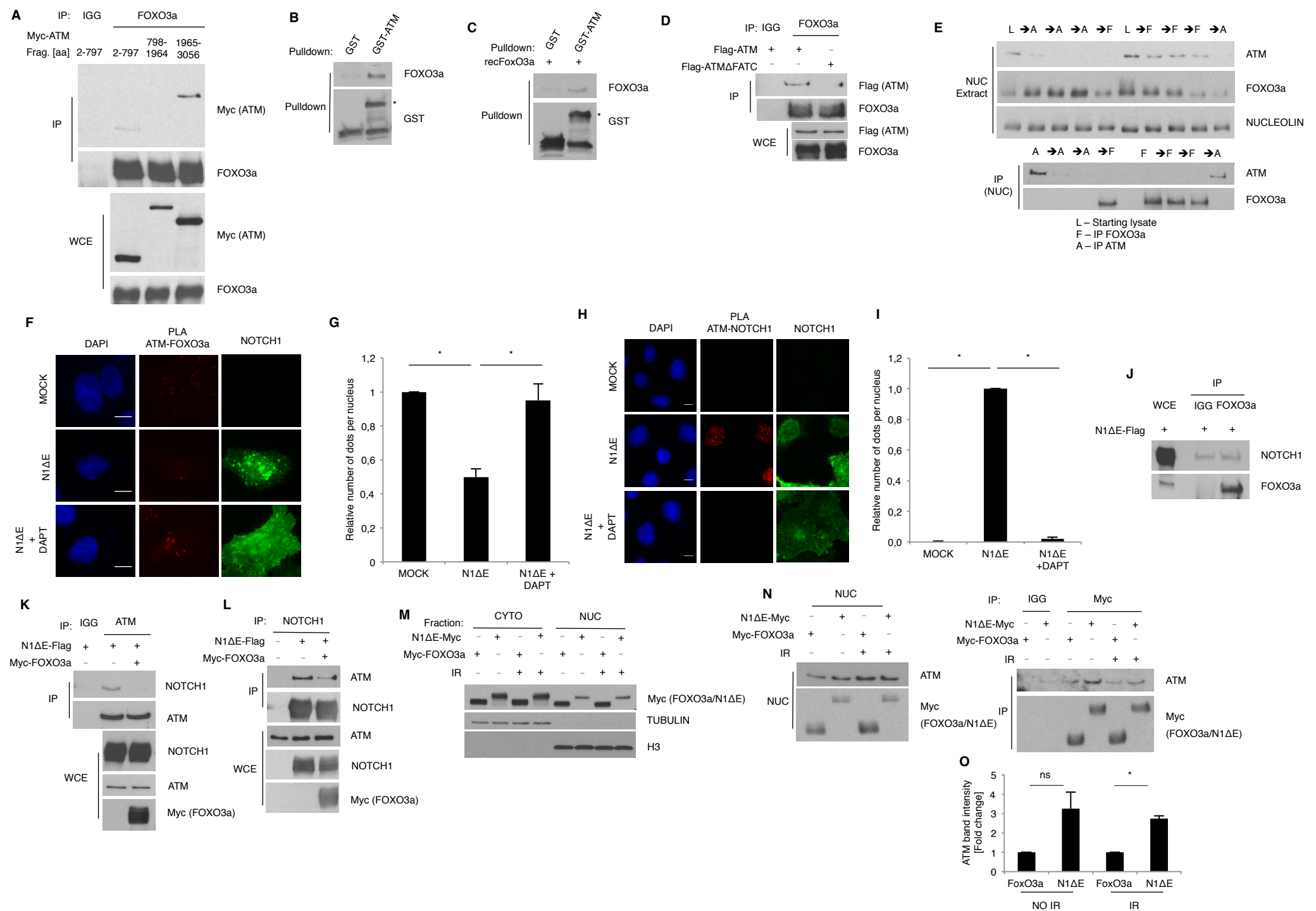
A
IP: IGG FOXO3a
Myc-ATM
Frag. [aa] 2-797 2-797 798-1964 1965-3056
IP
Myc (ATM)
FOXO3a
WCE
Myc (ATM)
FOXO3a
B
Pulldown: GST GST-ATM
Pulldown
FOXO3a
GST
C
Pulldown: GST GST-ATM
recFoxO3a + +
Pulldown
FOXO3a
GST
D
IP: IGG FOXO3a
Flag-ATM + + –
Flag-ATMΔFATC – – +
IP
Flag (ATM)
FOXO3a
WCE
Flag (ATM)
FOXO3a
E
L →A →A →A →F L →F →F →F →A
NUC Extract
ATM
FOXO3a
NUCLEOLIN
A →A →A →F F →F →F →A
IP (NUC)
ATM
FOXO3a
L – Starting lysate
F – IP FOXO3a
A – IP ATM
F
DAPI
PLA ATM-FOXO3a
NOTCH1
MOCK
N1ΔE
N1ΔE + DAPT
G
Relative number of dots per nucleus
1,2
1
0,8
0,6
0,4
0,2
0
*
*
MOCK
N1ΔE
N1ΔE + DAPT
H
DAPI
PLA ATM-NOTCH1
NOTCH1
MOCK
N1ΔE
N1ΔE + DAPT
I
Relative number of dots per nucleus
1,2
1,0
0,8
0,6
0,4
0,2
0,0
*
*
MOCK
N1ΔE
N1ΔE +DAPT
J
IP
WCE IGG FOXO3a
N1ΔE-Flag + + +
NOTCH1
FOXO3a
K
IP: IGG ATM
N1ΔE-Flag + + +
Myc-FOXO3a – – +
IP
NOTCH1
ATM
WCE
NOTCH1
ATM
Myc (FOXO3a)
L
IP: NOTCH1
N1ΔE-Flag – + +
Myc-FOXO3a – – +
IP
ATM
NOTCH1
WCE
ATM
NOTCH1
Myc (FOXO3a)
M
Fraction: CYTO NUC
N1ΔE-Myc – + – + – + – +
Myc-FOXO3a + – + – + – + –
IR – – + + – – + +
Myc (FOXO3a/N1ΔE)
TUBULIN
H3
N
NUC
N1ΔE-Myc – + – +
Myc-FOXO3a + – + –
IR – – + +
NUC
ATM
Myc (FOXO3a/N1ΔE)
IP: IGG Myc
N1ΔE-Myc – + – + – + – +
Myc-FOXO3a + – + – + – + –
IR – – – – + + + +
IP
ATM
Myc (FOXO3a/N1ΔE)
O
ATM band intensity [Fold change]
5
4
3
2
1
0
ns
*
FoxO3a N1ΔE FoxO3a N1ΔE
NO IR
IR

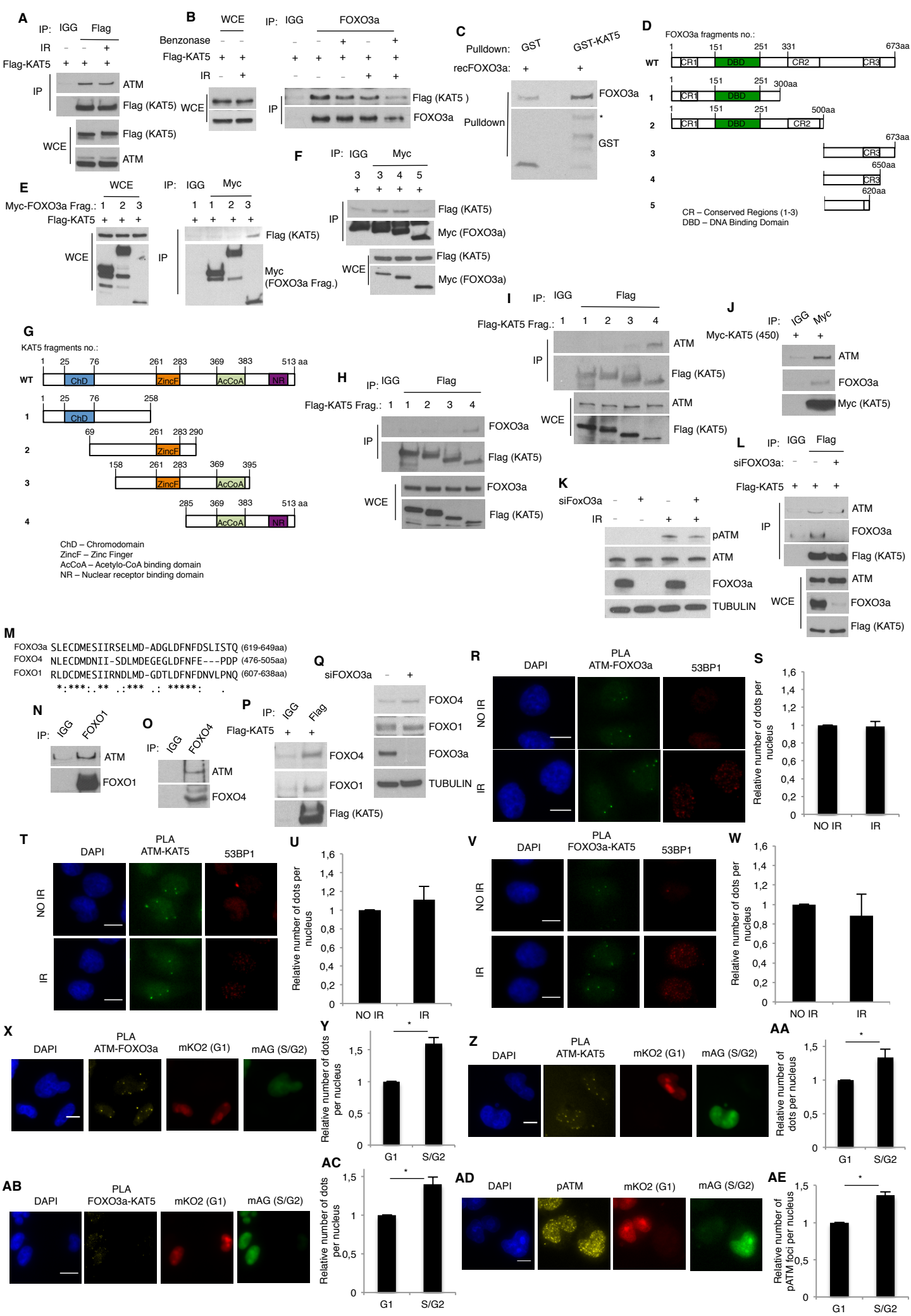
A
IP: IGG Flag
IR
Flag-KAT5
IP
ATM
Flag (KAT5)
WCE
Flag (KAT5)
ATM
B
WCE
Benzonase
Flag-KAT5
IR
WCE
IP: IGG FOXO3a
IP
Flag (KAT5)
FOXO3a
C
Pulldown: GST GST-KAT5
recFOXO3a:
Pulldown
FOXO3a
*
GST
D
FOXO3a fragments no.:
WT
CR1
DBD
CR2
CR3
673aa
300aa
500aa
650aa
620aa
CR – Conserved Regions (1-3)
DBD – DNA Binding Domain
E
WCE
Myc-FOXO3a Frag.:
Flag-KAT5
WCE
IP: IGG Myc
IP
Flag (KAT5)
Myc (FOXO3a Frag.)
F
IP: IGG Myc
IP
Flag (KAT5)
Myc (FOXO3a)
WCE
Flag (KAT5)
Myc (FOXO3a)
G
KAT5 fragments no.:
WT
ChD
ZincF
AcCoA
NR
513 aa
ChD – Chromodomain
ZincF – Zinc Finger
AcCoA – Acetylo-CoA binding domain
NR – Nuclear receptor binding domain
H
IP: IGG Flag
Flag-KAT5 Frag.:
IP
FOXO3a
Flag (KAT5)
WCE
FOXO3a
Flag (KAT5)
I
IP: IGG Flag
Flag-KAT5 Frag.:
IP
ATM
Flag (KAT5)
WCE
ATM
Flag (KAT5)
J
IP: IGG Myc
Myc-KAT5 (450)
ATM
FOXO3a
Myc (KAT5)
K
siFoxO3a
IR
pATM
ATM
FOXO3a
TUBULIN
L
IP: IGG Flag
siFOXO3a:
Flag-KAT5
IP
ATM
FOXO3a
Flag (KAT5)
WCE
ATM
FOXO3a
Flag (KAT5)
M
FOXO3a SLECDMESIIRSELMD-ADGLDFNFDSLISTQ (619-649aa)
FOXO4 NLECDMDNII-SDLMDEGEGLDFNFE---PDP (476-505aa)
FOXO1 RLDCDMESIIRNDLMD-GDTLDFNFDNVLPNQ (607-638aa)
*:***:.** .:*** .: *****: .
N
IP: IGG FOXO1
ATM
FOXO1
O
IP: IGG FOXO4
ATM
FOXO4
P
IP: IGG Flag
Flag-KAT5
FOXO4
FOXO1
Flag (KAT5)
Q
siFOXO3a
FOXO4
FOXO1
FOXO3a
TUBULIN
R
DAPI
PLA ATM-FOXO3a
53BP1
NO IR
IR
S
Relative number of dots per nucleus
NO IR
IR
T
DAPI
PLA ATM-KAT5
53BP1
NO IR
IR
U
Relative number of dots per nucleus
NO IR
IR
V
DAPI
PLA FOXO3a-KAT5
53BP1
NO IR
IR
W
Relative number of dots per nucleus
NO IR
IR
X
DAPI
PLA ATM-FOXO3a
mKO2 (G1)
mAG (S/G2)
Y
Relative number of dots per nucleus
*
G1
S/G2
Z
DAPI
PLA ATM-KAT5
mKO2 (G1)
mAG (S/G2)
AA
Relative number of dots per nucleus
*
G1
S/G2
AB
DAPI
PLA FOXO3a-KAT5
mKO2 (G1)
mAG (S/G2)
AC
Relative number of dots per nucleus
*
G1
S/G2
AD
DAPI
pATM
mKO2 (G1)
mAG (S/G2)
AE
Relative number of pATM foci per nucleus
*
G1
S/G2

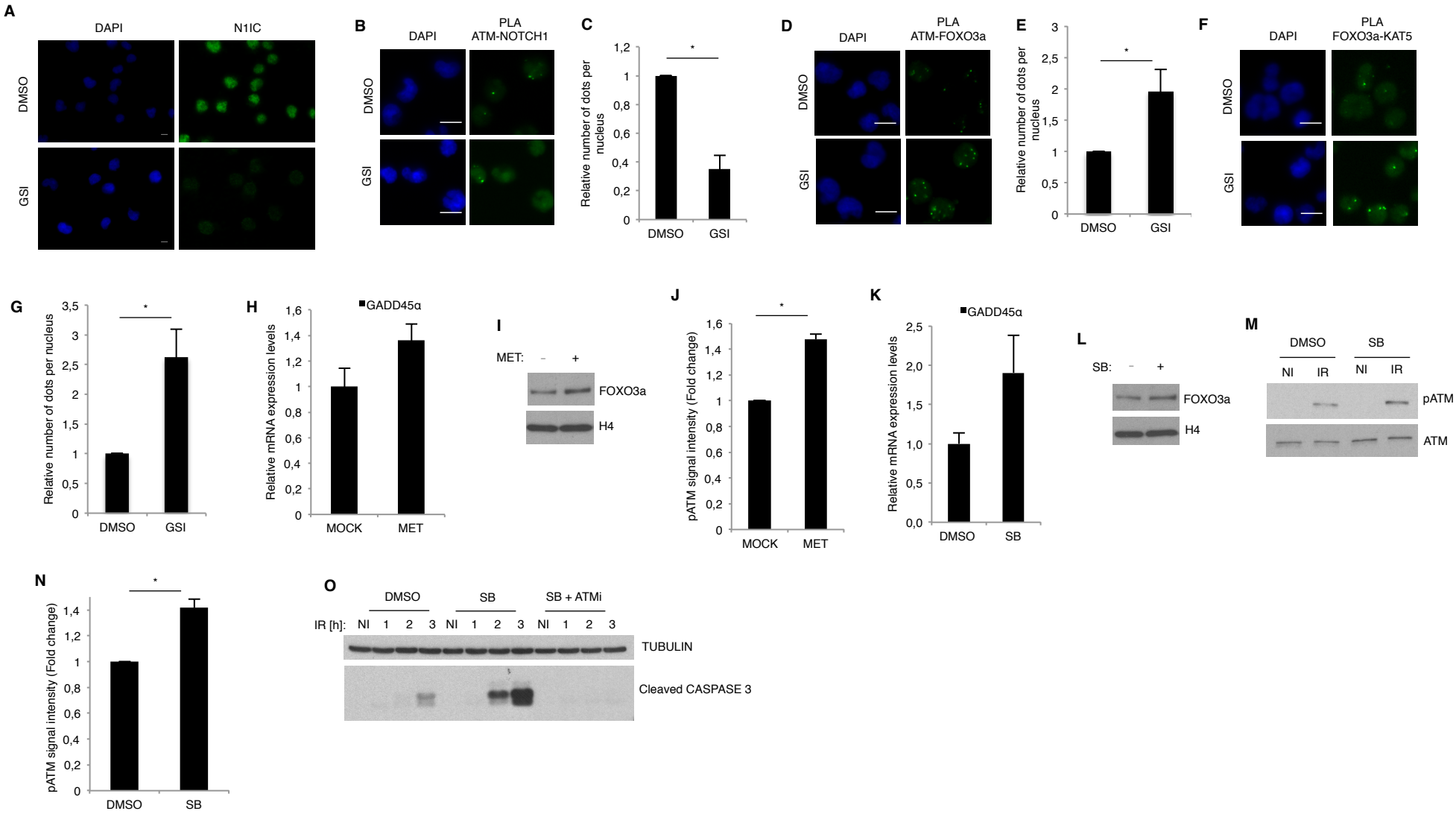
A
DAPI
N1IC
DMSO
GSI
B
DAPI
PLA ATM-NOTCH1
DMSO
GSI
C
Relative number of dots per nucleus
1,2
1
0,8
0,6
0,4
0,2
0
*
DMSO
GSI
D
DAPI
PLA ATM-FOXO3a
DMSO
GSI
E
Relative number of dots per nucleus
3
2,5
2
1,5
1
0,5
0
*
DMSO
GSI
F
DAPI
PLA FOXO3a-KAT5
DMSO
GSI
G
Relative number of dots per nucleus
3,5
3
2,5
2
1,5
1
0,5
0
*
DMSO
GSI
H
GADD45α
Relative mRNA expression levels
1,6
1,4
1,2
1
0,8
0,6
0,4
0,2
0
MOCK
MET
I
MET: – +
FOXO3a
H4
J
pATM signal intensity (Fold change)
1,6
1,4
1,2
1
0,8
0,6
0,4
0,2
0
*
MOCK
MET
K
GADD45α
Relative mRNA expression levels
2,5
2,0
1,5
1,0
0,5
0,0
DMSO
SB
L
SB: – +
FOXO3a
H4
M
DMSO
SB
NI
IR
NI
IR
pATM
ATM
N
pATM signal intensity (Fold change)
1,4
1,2
1
0,8
0,6
0,4
0,2
0
*
DMSO
SB
O
DMSO
SB
SB + ATMi
IR [h]: NI 1 2 3 NI 1 2 3 NI 1 2 3
TUBULIN
Cleaved CASPASE 3

Supplementary figure legends:

Supplementary Figure 1 - Related to Figure 2. NOTCH1 competes with FOXO3a for binding to the FATC domain of ATM.

(A) Immunoblot analysis of the coIP of the Myc-ATM fragments with FOXO3a.

(B) Immunoblot analysis of the pulldown experiment with the GST or GST-ATM (2842-3056aa) incubated with the lysate of HEK293T cells (asterisk indicates correct band).

(C) Immunoblot analysis of the pulldown experiment with GST or GST-ATM (2842-3056aa) incubated with the recombinant FOXO3a (asterisk indicates correct band).

(D) Immunoblot analysis of the coIP of Flag-ATM and Flag-ATMΔFATC with FOXO3a.

(E) Immunoblot analysis of the sequential immunodepletion of either ATM or FOXO3a. HEK293T cells were lysed and the nuclear fraction was subjected to sequential immunodepletions (L - starting lysate; F - immunodepletion of FOXO3a; A - immunodepletion of ATM).

(F) Immunofluorescence analysis of the PLA assay between ATM and FOXO3a in HeLa cells, expressing NOTCH1 and treated with GSI (Scale bar, 10μm).

(G) Analysis of the PLA shown in Fig.S1F. (Mean ± S.E.M.; n=3; two tailed Student's t-test; p value ≤0.05).

(H) Immunofluorescence analysis of the PLA assay between ATM and NOTCH1 in HeLa cells, expressing NOTCH1 and treated with GSI (Scale bar, 10μm).

(I) Analysis of the PLA shown in Fig.S1H (Mean ± S.E.M.; n=3; two tailed Student's t-test; p value ≤0.05).

(J) Immunoblot analysis of the coIP of NOTCH1 with FOXO3a.

(K) Immunoblot analysis of the coIP of NOTCH1 with ATM in cells over-expressing or not FOXO3a.

(L) Immunoblot analysis of the coIP of ATM with NOTCH1 in cells over-expressing or not FOXO3a.

(M) Immunoblot analysis of the expression levels of Myc-FOXO3a or N1ΔE-Myc. Cell lysate fractions: cytosolic (CYTO) and nuclear (NUC).

(N) Immunoblot analysis of the coIP of ATM with FOXO3a or NOTCH1, in cells expressing NOTCH1 or over-expressing FOXO3a from the nuclear fraction (NUC).

(O) Quantification of the immunoblots shown in Fig.S1N. ATM signal was normalized to Myc signal (Mean ± S.E.M.; n=2; two tailed Student's t-test; p value ≤0.05).

Supplementary Figure 2 - Related to Figure 3. FOXO3a bridges KAT5 binding to ATM.

(A) Immunoblot analysis of the coIP of ATM with KAT5.

(B) Immunoblot analysis of the coIP of KAT5 with FOXO3a.

(C) Immunoblot analysis of the pulldown experiments with GST or GST-KAT5 incubated with recombinant FOXO3a (asterisk indicates correct band).

(D) Scheme of the Myc-FOXO3a fragments used in this study.

(E) Immunoblot analysis of the coIP of KAT5 with Myc-FOXO3a fragments (1-3).

(F) Immunoblot analysis of the coIP of KAT5 with Myc-FOXO3a fragments (3-5).

(G) Scheme of Flag-KAT5 fragments used in this study.

(H) Immunoblot analysis of the coIP of FOXO3a with Flag-KAT5 fragments (1-4).

(I) Immunoblot analysis of the coIP of ATM with Flag-KAT5 fragments (1-4).

(J) Immunoblot analysis of the coIP of FOXO3a and ATM with Myc-KAT5 fragment (450-513aa).

(K) Immunoblot analysis of the ATM activation (pATM) in HeLa cells transfected with siRNA against *FOXO3a* or *LUCIFERASE* (2G; 1h).

(L) Immunoblot analysis of the coIP of ATM and FOXO3a with KAT5 in HEK293T cells transfected with siRNA against *FOXO3a* or *LUCIFERASE* and Flag-KAT5 construct.

(M) Protein alignment of the human FOXO3a, human FOXO4 and human FOXO1 done in clustal X. "*" - fully conserved residue. ":" - strongly similar properties of the residues. "." - weakly similar properties of the residues

(N) Immunoblot analysis of coIP of ATM with FOXO1.

(O) Immunoblot analysis of coIP of ATM with FOXO4.

(P) Immunoblot analysis of the coIP of FOXO1 and FOXO4 with KAT5. HEK293T cells were transfected with Flag-KAT5 construct.

(Q) Immunoblot analysis of the proteins levels (FOXO1 and FOXO4) in HEK293T cells transfected with siRNA against *FOXO3a* or *LUCIFERASE.*

(R) Immunofluorescence analysis of the PLA assay between ATM and FOXO3a in HeLa cells (Scale bar, 10μm).

(S) Analysis of the PLA shown in Fig.S2R. (Mean ± S.E.M.; n=3).

(T) Immunofluorescence analysis of the PLA assay between ATM and KAT5 in HeLa cells (Scale bar, 10μm).

(U) Analysis of the PLA shown in Fig.S2T. (Mean ± S.E.M.; n=3).

(V) Immunofluorescence analysis of the PLA assay between FOXO3a and KAT5 in HeLa cells (Scale bar, 10μm).

(W) Analysis of the PLA shown in Fig.S2V. (Mean ± S.E.M.; n=3).

(X) Immunofluorescence analysis of the PLA assay between ATM and FOXO3a in HeLa Fucci cells (Scale bar, 10μm).

(Y) Analysis of the PLA shown in Fig.S2X. (Mean ± S.E.M.; n=3; two tailed Student's t-test; p value ≤0.05).

(Z) Immunofluorescence analysis of the PLA assay between ATM and KAT5 in HeLa Fucci cells (Scale bar, 10μm).

(AA) Analysis of the PLA shown in Fig.S2Z. (Mean ± S.E.M.; n=3; two tailed Student's t-test; p value ≤0.05).

(AB) Immunofluorescence analysis of the PLA assay between FOXO3a and KAT5 in HeLa Fucci cells (Scale bar, 10μm).

(AC) Analysis of the PLA shown in Fig.S2AB. (Mean ± S.E.M.; n=3; two tailed Student's t-test; p value ≤0.05).

(AD) Immunofluorescence analysis of the ATM activation (pATM) in HeLa Fucci cells (Scale bar, 10μm).

(AE) Analysis of the immunofluorescence shown in Fig.S2AD. (Mean ± S.E.M.; n=3; two tailed Student's t-test; p value ≤0.05).

Supplementary Figure 3 - Related to Figure 4. Induction of FOXO3a nuclear localization sensitizes T-ALL cells to DNA damage induced cell death.

(A) Immunofluorescence analysis of the NOTCH1 localization in CUTLL1 cells treated with GSI (Scale bar, 10μm). N1IC - nuclear form of NOTCH1.

(B) Immunofluorescence analysis of the PLA assay between ATM and NOTCH1 in CUTLL1 cells treated GSI (Scale bar, 10μm).

(C) Analysis of the PLA shown in Fig.S3B. (Mean ± S.E.M.; n=3; two tailed Student's t-test; p value ≤0.05)

(D) Immunofluorescence analysis of the PLA assay between ATM and FOXO3a in CUTLL1 cells treated with GSI (Scale bar, 10μm).

(E) Analysis of the PLA shown in Fig.S3D. (Mean ± S.E.M.; n=4; two tailed Student's t-test; p value ≤0.05)

(F) Immunofluorescence analysis of the PLA assay between FOXO3a and KAT5 in CUTLL1 cells treated with GSI (Scale bar, 10μm).

(G) Analysis of the PLA shown in Fig.S3F. (Mean ± S.E.M.; n=4; two tailed Student's t-test; p value ≤0.05).

(H) qRT-PCR quantification of the mRNA expression levels of *GADD45α* in TALL-1 cells treated with MET. Values were normalized to the expression levels of *B2M* (unrelated gene).

(I) Immunoblot analysis of the FOXO3a nuclear localization upon treatment of TALL-1 cells with MET. TALL-1 cell were lysed and chromatin fraction of the lysate was extracted.

(J) Quantification of the signals shown in Fig.4A. pATM signal was normalized to ATM (Mean ± S.E.M.; n=3; two tailed Student's t-test; p value ≤0.05).

(K) qRT-PCR quantification of the mRNA expression levels of *GADD45α* , in TALL-1 cells treated with SB. Values were normalized to the expression levels of *B2M* (unrelated gene).

(L) Immunoblot analysis of the FOXO3a nuclear localization upon treatment of TALL-1 cells with SB. TALL-1 cell were lysed and chromatin fraction of the lysate was extracted.

(M) Immunoblot analysis of the ATM activation (pATM) in TALL-1 cells pretreated with SB.

(N) Quantification of the signals shown in Fig.S3M. pATM signal was normalized to ATM (Mean ± S.E.M.; n=4; two tailed Student's t-test; p value ≤0.05).

(O) Immunoblot analysis of the DNA damage-induced cell death (cleaved CASPASE 3) in TALL-1 cells pretreated with SB or SB and ATM inhibitor (ATMi).

Supplementary Table 1

Antibody:	Provider:	Use:	Cat. No.:	Species:
ATM	Abcam	WB 1:6000 5% Milk	ab32420	Rabbit
ATM	Sigma	WB 1:6000 5% Milk IP 1: 500 IF 1:200	A1106	Mouse
53BP1	Bethyl	IF 1:4000	A303906A	Goat
Celavaded CASPASE 3	Cell Signaling	WB: 1:1000 5% BSA	9661	Rabbit
pATM (S1981)	Rockland	WB 1:6000 5%Milk IF 1:200	200-301-400	Mouse
NOTCH1	Santa Cruz	WB 1:1000 5% Milk IF: 1:200	sc-6014	Goat
N1IC	Cell Signaling	IF: 1:200	4147S	Rabbit
GFP	Santa Cruz	WB 1:6000 5% Milk	sc-9996	Mouse
Flag	Sigma	WB 1:6000 5% Milk IP 1:500	F1804	Mouse
Flag	Cell Signaling	WB 1:6000 5% Milk	2368	Rabbit
Myc	Santa Cruz	WB 1:6000 5% Milk IP 1:500	sc-40	Mouse
Myc	Cell Signaling	WB 1:6000 5% Milk	2272	Rabbit
FOXO3a	Cell Signaling	IF 1:200	2497	Rabbit

FOXO3	Sigma	IF 1:200	SAB1403829	Mouse
FOXO3a	Abcam	WB 1:6000 5% Milk	ab109629	Rabbit
FOXO3a	Santa Cruz	IP 1:50	sc-11351	Rabbit
FOXO1	LifeSpan BioSciences	WB 1:8000 5% Milk IP 1:250	LS-C287207	Rabbit
FOXO4	Abcam	WB 1:8000 5% Milk IP 1:500	Ab128908	Rabbit
KAT5	Santa Cruz	WB 1:1000 5% Milk IP 1:30	sc-5725	Goat
KAT5	Kind gift of B. Amati	WB 1:1000 5% Milk IF 1:200	x	Rabbit
KAT5	LifeSpan BioSciences	WB 1:5000 5% Milk	LS-C109474	Rabbit
GST	Biochemistry Facility, IFOM-IEO Campus	WB 1:8000 5% Milk	x	Rabbit
NBS1	Novus	WB 1:1000 5% Milk IP 1:500	NB 100-143	Rabbit
TUBULIN	Sigma	WB 1:8000 5% Milk	T6074	Mouse
H3	Abcam	WB 1:8000 5% Milk	ab10799	Mouse
H4	Abcam	WB 1:8000 5% Milk	Ab10158	Rabbit
NUCLEOLIN	Novus	WB 1:8000 5% Milk	NB 600-241	Rabbit

WB - Western Blot; IF - Immunofluorescence; IP - Immunoprecipitation

Supplementary Table 2

Primers used:	Sequence (5'->3'):
qRT-PCR:	
GADD45α	Fr TTTGCAATATGACTTTGGAGGA
	Rv CATCCCCCACCTTATCCAT
B2M	Fr TTCTGGCCTGGAGGCTATC
	Rv TCAGGAAATTTGACTTTCCATTC
Cloning:	
GST-KAT5	Fr GATCGGATCCATGGCGGAGG
	Rv GATCGTCGACTCACCACTTCCC
Myc-FoxO3a 1-300	Fr GATCGGATCCATGGCAGAGGCACCGG
	Rv GATCCTCGAGTCAACTGCTGCGTGACGTGGG
Myc-FoxO3a 1-500	Fr GATCGGATCCATGGCAGAGGCACCGG
	Rv GATCCTCGAGTCACACAGCGGTGCTGGCC
Myc-FoxO3a 500-673	Fr GATCGGATCCATGTCTGCCCAGAATTCCC
	Rv GATCCTCGAGTCAGCCTGGCACCCAG
Myc-FoxO3a 500-650	Fr GATCGGATCCATGTCTGCCCAGAATTCCC
	Rv GATCCTCGAGTCAATTCTGTGTGGAGATGAGGG
Myc-FoxO3a 500-620	Fr GATCGGATCCATGTCTGCCCAGAATTCCC
	Rv GATCCTCGAGTCACAAGCTCCCATTGAAC
Myc-KAT5 450-513	Fr GATCGGATCCAAGAAGGAGGATG
	Rv GATCCTCGAGTCACCACTTCCC
GST-FOXO3a	Fr GATCGGATCCATGGCAGAGGCAC
	Rv GATCGTCGACTCAGCCTGGCAC

FRANK, S. R., PARISI, T., TAUBERT, S., FERNANDEZ, P., FUCHS, M., CHAN, H.-M. M., LIVINGSTON, D. M. & AMATI, B. 2003. MYC recruits the TIP60 histone acetyltransferase complex to chromatin. *EMBO reports,* 4**,** 575-580.

KAIDI, A. & JACKSON, S. P. 2013. KAT5 tyrosine phosphorylation couples chromatin sensing to ATM signalling. *Nature,* 498**,** 70-4.

KHANNA, K. K., KEATING, K. E., KOZLOV, S., SCOTT, S., GATEI, M., HOBSON, K., TAYA, Y., GABRIELLI, B., CHAN, D., LEES-MILLER, S. P. & LAVIN, M. F. 1998. ATM associates with and phosphorylates p53: mapping the region of interaction. *Nat Genet,* 20**,** 398-400.

KIM, M. Y., ANN, E. J., KIM, J. Y., MO, J. S., PARK, J. H., KIM, S. Y., SEO, M. S. & PARK, H. S. 2007. Tip60 histone acetyltransferase acts as a negative regulator of Notch1 signaling by means of acetylation. *Mol Cell Biol,* 27**,** 6506-19.

PARK, S., KANG, J. M., KIM, S. J., KIM, H., HONG, S., LEE, Y. J. & KIM, S. J. 2015. Smad7 enhances ATM activity by facilitating the interaction between ATM and Mre11-Rad50-Nbs1 complex in DNA double-strand break repair. *Cell Mol Life Sci,* 72**,** 583-96.

VERMEZOVIC, J., ADAMOWICZ, M., SANTARPIA, L., RUSTIGHI, A., FORCATO, M., LUCANO, C., MASSIMILIANO, L., COSTANZO, V., BICCIATO, S., DEL SAL, G. & D'ADDA DI FAGAGNA, F. 2015. Notch is a direct negative regulator of the DNA-damage response. *Nat Struct Mol Biol,* 22**,** 417-24.

WANG, F., MARSHALL, C. B., YAMAMOTO, K., LI, G. Y., PLEVIN, M. J., YOU, H., MAK, T. W. & IKURA, M. 2008. Biochemical and structural characterization of an intramolecular interaction in FOXO3a and its binding with p53. *J Mol Biol,* 384**,** 590-603.